Intrinsic magnetic order and inhomogeneous transport in Gd-implanted zinc oxide

John Kennedy,[1,2,*] Grant V. M. Williams,[2] Peter P. Murmu,[1,2] and Ben J. Ruck[2]
[1]*National Isotope Centre, GNS Science, P.O. Box 31312, Lower Hutt 5010, New Zealand*
[2]*The MacDiarmid Institute for Advanced Materials and Nanotechnology, School of Chemical and Physical Sciences, Victoria University of Wellington, P.O. Box 600, Wellington 6140, New Zealand*
(Received 2 September 2013; published 23 December 2013)

We report the results from magnetic, resistivity, and Hall effect measurements on a ferromagnetically ordered 5% Gd low energy implanted ZnO single crystal. Temperature-dependent magnetization measurements show that the Gd ions do not contribute to the magnetic order; hence, the magnetic order is intrinsic. The electronic transport in the Gd-implanted region is inhomogeneous, and there is a nonlinear Hall resistance. The nonlinear Hall resistance is likely to be a consequence of the inhomogeneous transport and not due to an anomalous Hall effect.

DOI: 10.1103/PhysRevB.88.214423 PACS number(s): 71.55.Gs, 75.50.Pp

Dilute magnetic semiconductors (DMS) remain in the forefront of spin polarized electronics (spintronics) research because of the potential for new devices. In a typical DMS system, the ferromagnetic order is established via charge carriers. For example, Dietl *et al*. reported hole mediated ferromagnetic order in Mn-doped GaAs.[1] However, ferromagnetism has also been reported in a series of DMS materials that show poor electrical conductivity.[2] The appearance of an anomalous Hall effect (AHE) is sometimes used as evidence for a DMS. For example, Behan *et al*.[3] and Hsu *et al*.[4] observed an AHE in metallic or semiconducting Co- or Mn-doped ZnO. However, an AHE was reported in Co-doped $TiO_{2-\delta}$ even though it contained superparamagnetic Co nanoparticles.[5] An AHE was also observed in ZnO:Cu films that showed no evidence for ferromagnetic order, and the magnitude of the AHE was similar to that found in a ferromagnetically ordered ZnO film.[6] This suggests that the observation of an AHE effect is not necessarily evidence for a DMS.

There are a number of reports of ferromagnetism in undoped,[6–14] transition metal,[15–17] or rare earth doped[18–22] ZnO. In the case of undoped ZnO, the ferromagnetism was attributed to intrinsic point defects (Zn or oxygen vacancies)[6–13] or extended defects at the surface or grain boundaries.[14] Ferromagnetism in transition-metal doped ZnO is believed to be due to the formation of a transition metal band and double exchange.[15] Ferromagnetism in rare earth doped ZnO can occur via a carrier mediated mechanism.[19–23] It has been reported that this can account for the large ordered moment observed in ZnO:Gd of up to 3274 μ_B per Gd,[19] where μ_B is the Bohr magneton, although much lower ordered moments of up to 1.8 μ_B per Gd[21] and 0.06 μ_B per Gd[19] have also been reported. However, no magnetic order was observed in ZnO:Gd films made by magnetron sputtering,[22] and it was concluded from an *ab initio* study[24,25] that Gd cannot induce the required electronic polarization to ferromagnetically order the Gd moments. We have recently shown that ferromagnetism can be observed in hydrothermally grown ZnO crystals.[18] The saturation magnetic moment was not correlated with the Gd concentration; hence it may be that the ferromagnetism arises from point defect nanoclusters near the surface. However, it was not possible to completely exclude the formation of ferromagnetic Gd nanoparticles because the Curie temperature of Gd metal is 294 K (Ref. 26), which is close to the Curie temperature found in our low energy Gd-implanted ZnO crystals. Khalid and Esquinazi[27] recently reported ferromagnetic order in low energy hydrogen-implanted ZnO crystals, where there was an enhancement of the saturation moment with increasing hydrogen fluence. An AHE was observed, but it did not follow the magnetization data except at and above 220 K. This suggests that the departure from linearity of the Hall resistivity below 220 K is caused by some other effect and is not due to an AHE.

In this paper, we report the results from magnetic, resistivity, and Hall effect measurements on a low energy 5% Gd-implanted and 650 °C annealed ZnO hydrothermally grown single crystal ($Zn_{0.95}Gd_{0.05}O$). We show that the Gd ions do not form magnetically ordered clusters and that the resistivity can be modeled using the Khalid and Esquinazi model,[27] where there is inhomogeneous transport near the surface. We also observe a nonlinear Hall resistivity that is likely to be a consequence of the inhomogeneous transport rather than being due to an AHE.

Hydrothermally grown ZnO (0001) crystals obtained from Semi-Wafer, Inc. were implanted with 40 keV Gd ions. The Gd fluence was 6.4×10^{15} ions cm^{-2}, resulting in a 5 at.% Gd concentration in the near-surface region. The implanted samples were annealed in a high vacuum chamber ($\sim 10^{-7}$ mbar) at 650 °C for 30 minutes. The magnetic properties were investigated using a Magnetic Property Measurement System (MPMS) employing a superconducting quantum interference device (SQUID) magnetometer. Resistivity and Hall effect measurements were made using a Physical Property Measurement System (PPMS).

We show in Fig. 1 the moment per unit area, m', as a function of temperature at 1 T. There is a large upturn at low temperatures that arises from Gd^{3+} moments as well as point defect moments that are not involved in the magnetic order. There is also a contribution from the ordered magnetic defect nanoclusters and a diamagnetic contribution that is dominated by the unimplanted ZnO region. It is also possible that there are some Gd ions that form magnetically ordered Gd nanoparticles. For this reason we modeled the magnetic data using

$$m' = m'_{Gd} + m'_D + \chi_0 Bt/\mu_0 + m'_S, \quad (1)$$

where m'_{Gd} is the paramagnetic contribution from paramagnetic Gd^{3+}, and it can arise from distributed Gd^{3+} ions or from paramagnetic Gd_2O_3. m'_D is the paramagnetic contribution

 ©2013 American Physical Society

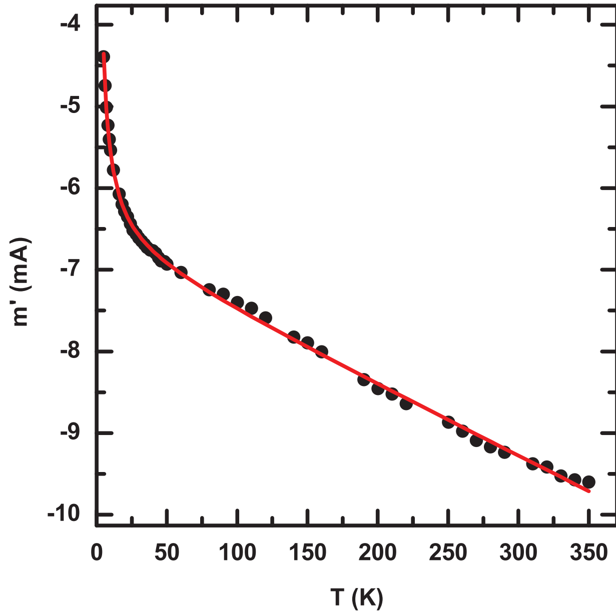

FIG. 1. (Color online) Temperature-dependent moment per unit area, m', for $Zn_{0.95}Gd_{0.05}O$ at 1 Tesla (filled circles). The solid curve is a fit to the data using Eqs. (1)–(3).

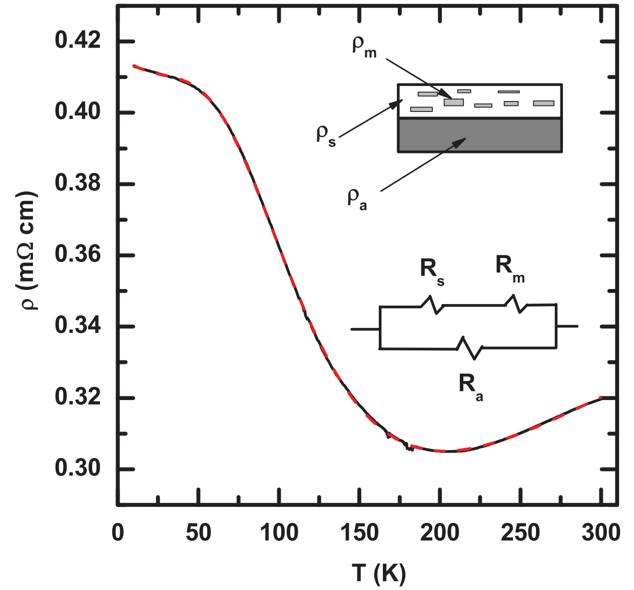

FIG. 2. (Color online) Temperature-dependent resistivity for $Zn_{0.95}Gd_{0.05}O$ (solid curve). The dashed curve is a fit to the data using Eq. (4). Also shown in is a schematic of inhomogeneous resistivity model with normal metallic ρ_m, semiconducting ρ_s, and disordered ρ_a resistivities (upper) and the resistance network used to model the data (lower).

from the point defects, χ_0 is the ZnO core diamagnetic susceptibility, and m'_S is the saturation moment per unit area from the ordered moments. m'_S is known to be significantly less at room temperature[18]; hence, we model this contribution as being linear with increasing temperature. $m'_{\rm Gd}$ is determined by the Brillouin function, where $m'_{\rm Gd}$ can be written as

$$m'_{\rm Gd} = n'_{\rm Gd} g \mu_{\rm B} J \left[\frac{2J+1}{2J} \coth\left(\frac{2J+1}{2J}x\right) - \frac{1}{2J}\coth\left(\frac{x}{2J}\right)\right], \tag{2}$$

where $n'_{\rm Gd}$ is the paramagnetic Gd^{3+} concentration per unit area, $g = 2$, and $J = 7/2$ for the $^8S_{7/2}$ ground state. $x = g\mu_B JB/(k_B T)$, where B is the magnetic field, k_B is Boltzmann's constant, and T is the temperature. We assume that the point defect paramagnetic moment is low; hence, it is reasonable to use the Curie term for m'_D and hence,

$$m'_D = \frac{n'_D P_{\rm eff}^2 \mu_{\rm B}^2 B}{3k_{\rm B} T}, \tag{3}$$

where n'_D is the point defect concentration per unit area, and $P_{\rm eff}$ is the effective moment divided by μ_B.

We show in Fig. 1 that the data can be fitted using the functions above and with $n'_{\rm Gd}$ being the implanted Gd^{3+} concentration and $n'_D \times P_{\rm eff}{}^2$ of 2.1×10^{21} $\rm m^{-2}$. This shows that the data can be modeled with all of the Gd^{3+} ions being paramagnetic and without a fraction of the Gd ions forming magnetically ordered Gd nanoparticles. If the paramagnetic point defects were F centers with $S = ½$, then $P_{\rm eff} = 1.73$. Thus, $n'_D \times P_{\rm eff}{}^2 = 2.1 \times 10^{21}$ $\rm m^{-2}$ would imply that $n'_D = 7.0 \times 10^{20}$ $\rm m^{-2}$. This assumption is supported by measurements by Zhan *et al.* on thermally annealed ZnO films in Ar.[11] They deduced a magnetic moment from a singly occupied oxygen vacancy and suggested that they were responsible for the ferromagnetism. It is unlikely that the paramagnetic point defects are in the same region near the surface where superparamagnetism occurs. We previously showed that superparamagnetism occurs in the Gd ion-implanted thickness of 40 nm (Ref. 18). If the defect paramagnetic moment was in this Gd-implanted region, then the defects would on average be separated by 3.8 Å, which is not possible. However, if the paramagnetic point defects were throughout the crystal (0.5 mm thick), then the average separation is 89 Å. Since the volume per ZnO is 23.4 $Å^3$ (Ref. 28), this would imply a slightly reduced ZnO crystal with a 0.0017% oxygen deficiency. This is possible, and oxygen deficiencies of up to 1% have been reported in the literature.[29]

The electrical resistivity is plotted in Fig. 2, and the data were obtained using the Gd implantation depth of 40 nm. We first note that the unimplanted magnetically ordered ZnO crystal resistivity is very high, and it is reduced by six orders of magnitude after Gd implantation, which implies that Gd implantation leads to significant carrier doping. The increase in the resistivity below ~200 K appears to suggest a metal-semiconductor-like transition that has also been reported from other measurements on ZnO films[30] and hydrogen-doped ZnO films[31] that do not display magnetic order. In both cases the resistivity was modeled in terms of weak localization and Coulomb electron interactions as well as another high temperature T^2 term. However, the resultant resistivity model does not provide a good fit to our data over the entire temperature range because our resistivity data starts to saturate below ~55 K.

We note that the temperature dependence of our resistivity data is similar to that reported by Khalid and Esquinazi[27] from measurements on hydrogen-implanted ZnO crystals where the

resistivity decreases until ∼220 K and then increases with decreasing temperature and starts to saturate below ∼50 K. One key difference is that the resistivity has only increased by 29% in our Gd-implanted sample at low temperature, while it has increased by at least two orders of magnitude in hydrogen-implanted ZnO. However, we find that we can model our resistivity data using their inhomogeneous model, which is illustrated in the upper inset to Fig. 2. There is one layer containing metallic islands with resistivity ρ_m embedded in a semiconducting region with resistivity ρ_s. The metallic islands could possibly be related to superparamagnetic defect clusters that have been reported to occur near the surface.[18] For $Zn_{0.95}Gd_{0.05}O$, there is a broad plateau in the zero-field-cooled data between 51 K and 120 K, which is indicative of a distribution in superparamagnetic cluster sizes.[18] There is also another disordered layer with a resistivity ρ_a. Similar to the hydrogen-implantation study,[27] we also approximate the resistance (see the lower inset in Fig. 2) in this inhomogeneous model by

$$R = \left(\frac{1}{R_a} + \frac{1}{R_m + R_s}\right)^{-1}, \quad (4)$$

where R_m is the metallic resistance, R_s is the semiconducting resistance, and R_a is the disordered layer resistance. The normal state resistance is modeled as $R_m = R_{m0} + R_{m1} \times T^{n1}$ to account for the usual observation that metallic resistances can have exponents that vary from 1 to 2. The semiconducting resistance was modeled as being thermally activated, where $R_s = R_{s0} \times \exp(\Delta/(k_B T))$ and Δ is the activation energy. The disordered layer resistance is modeled as $R_a = R_{a0} - R_{a1} \times T^{n2}$. The best fit using Eq. (4) is plotted in Fig. 2. We find an activation energy of 54 meV, which is close to the 60 meV found in low energy hydrogen-implanted ZnO (Ref. 27). The fit also produced a nearly temperature-independent R_a, which is consistent with the assumption that the corresponding region is disordered.

It is apparent in Fig. 3 that the Hall resistance is not linear with the applied magnetic field at 100 K. This may suggest the appearance of an AHE, which we discuss later. In this case the Hall resistance, R_{xy}, can be written as

$$R_{xy} = \frac{R_H B}{t} + R_{xy\text{-}NL}, \quad (5)$$

where R_H is the Hall coefficient, t is the thickness, and $R_{xy\text{-}NL}$ is the nonlinear contribution to the Hall resistance. For homogeneous and simple metals or semiconductors, $R_H = -1/(ne)$, where n is the carrier concentration. We plot the resultant n in the inset to Fig. 3, where we have used the high field gradient of R_{xy} to estimate R_H and t is the implantation depth of 40 nm. The room temperature n values are comparable to those reported in other studies.[27,32] However, we find that the temperature dependence of n appears to be similar to the resistivity plotted in Fig. 2, where n initially decreases with decreasing temperature and then increases below ∼200 K. The temperature dependence of n may be because in the model used to obtain Eq. (4) the current transport is predominately through the R_a region at low and high temperatures. This can result in similar carrier concentrations at low and high temperatures. In the intermediate temperature region there is also significant

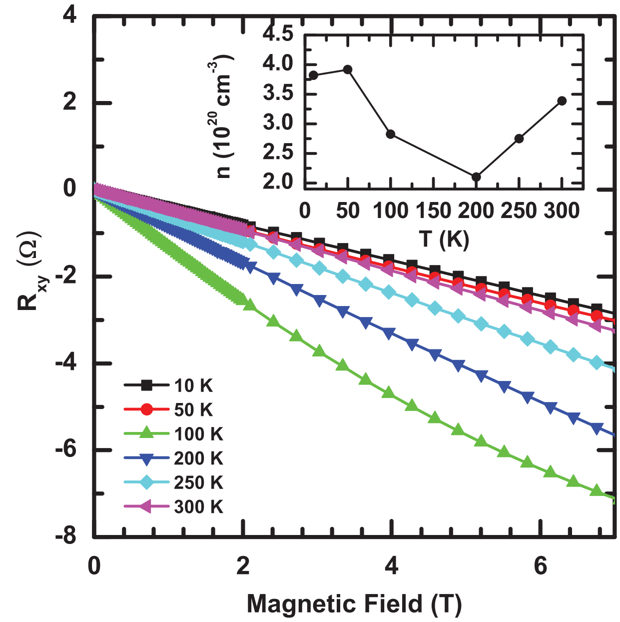

FIG. 3. (Color online) Hall resistance for $Zn_{0.95}Gd_{0.05}O$ with a current of 0.1 mA. Inset: the carrier concentration estimated from the Hall data.

transport in the R_m and R_s regions. This can lead to a change in n calculated from R_H in the intermediate temperature region.

If $R_{xy\text{-}NL}$ arises from an AHE, then it can be written as $R_{xy\text{-}NL} = R_s M/t$, where R_s the AHE coefficient and M is the magnetization. We show in Fig. 4(a) that $R_{xy\text{-}NL}$ is still increasing even at 7 T. This is not expected because the magnetization from the ferromagnetically ordered moments

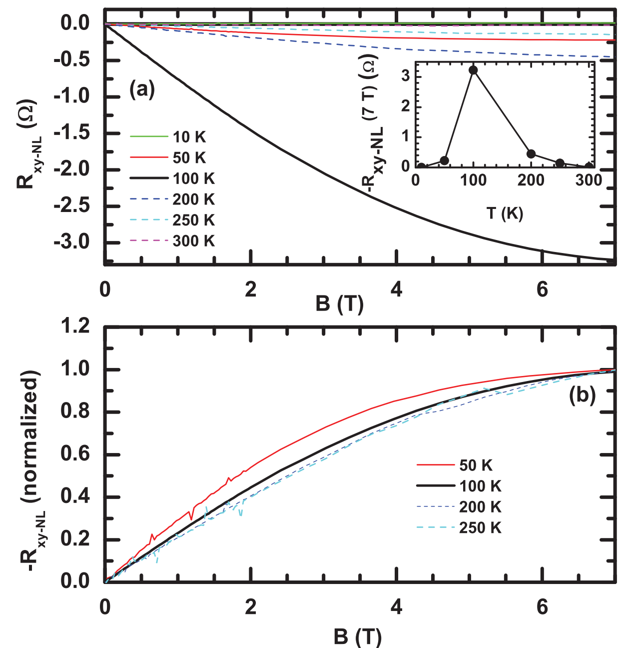

FIG. 4. (Color online) (a) The nonlinear contribution to the Hall resistance, $R_{xy\text{-}NL}$, for $Zn_{0.95}Gd_{0.05}O$ at different temperatures. Inset: Plot of $-R_{xy\text{-}NL}$ at 7 T against temperature. (b) $-R_{xy\text{-}NL}$ normalized to the same value at 7 T.

saturates at ∼0.4 T (Ref. 18). The magnetic field dependence of $R_{xy\text{-}NL}$ is similar to that reported from the study of hydrogen-implanted ZnO at 40 K and below although the sign of $R_{xy\text{-}NL}$ is different.[27] However, this study also reported a $R_{xy\text{-}NL}$ that systematically decreased with increasing temperature and a different magnetic field dependence of $R_{xy\text{-}NL}$ at higher temperatures where only $R_{xy\text{-}NL}$ at and above 225 K followed the magnetic field dependence expected from an AHE. In our case, low energy Gd implantation results in a large negative $R_{xy\text{-}NL}$ at 100 K, which is seen more clearly in the inset to Fig. 4(a) where $-R_{xy\text{-}NL}$ is plotted at 7 T and as a function of temperature. Furthermore, the dependence of $R_{xy\text{-}NL}$ on B has nearly the same functional form from 50 K to 250 K, as can be seen in the normalized $-R_{xy\text{-}NL}$ plotted in Fig. 4(b). $R_{xy\text{-}NL}$ at 300 K is too small and noisy to be included in the figure. However, it does not follow the magnetization. The 10 K data are also small and noisy and shows a small and positive $R_{xy\text{-}NL}$.

It is possible that $R_{xy\text{-}NL}$ does not follow the expected dependence on the magnetization because of the inhomogeneous transport. We note that a nonlinear R_{xy} was also observed from recent modeling of magnetotransport in inhomogeneous conductors using an array of coupled four-terminal elements.[33] Thus, different electronic transport mechanisms in the metallic superparamagnetic nanoclusters, the semiconducting region, and the disordered region could lead to a nonlinear R_{xy} that does not follow the magnetization. The large apparent $R_{xy\text{-}NL}$ at 100 K may simply be because the electronic transport in this temperature region has a significant contribution from R_s and R_a.

The inhomogeneous transport explanation could also explain the apparent anomalous Hall voltage found in ferromagnetic Ni and Co ferrite nanoparticles in ZnO induced by ion implantation and vacuum annealing where the apparent anomalous Hall voltage does not saturate at 6 T while the magnetization saturates below ∼0.5 T (Ref. 34). It could also explain the apparent anomalous Hall resistivity found in $Zn_{0.985}Cu_{0.015}O$ films that do not show evidence for magnetic order.[35] It is possible that the apparent anomalous Hall resistance that does not follow the magnetization at and below 200 K in low energy hydrogen-implanted ZnO (Ref. 27) may also be due to inhomogeneous transport. At higher temperatures (above ∼200 K), the semiconducting resistivity contribution to the resistivity does not appear to be large; the resistivity is below 100 $\mu\Omega$ cm, and $R_{xy\text{-}NL}$ is ∼3 mΩ (cf. ∼−14 mΩ at 300 K in our sample). This may be why an AHE that follows the magnetization is observed at high temperatures in low energy hydrogen-implanted ZnO.

In conclusion, we have shown that the magnetic data from a ferromagnetically ordered low energy Gd-implanted hydrothermally grown ZnO crystal can be modeled by noninteracting Gd^{3+} moments, a ferromagnetic contribution, a paramagnetic contribution from intrinsic defects throughout the ZnO crystal, and a diamagnetic contribution. This shows that the implanted Gd ions are not ferromagnetically ordered, and it is consistent with our previous study[18] where we found that the saturation magnetic moment was not correlated with the Gd concentration. The absence of ordered Gd moments means that the ferromagnetic order is intrinsic and likely to arise from superparamagnetic defect clusters near the surface of the crystal. The resistivity data shows a metal-semiconductor-like transition at ∼200 K and can be modeled using the Khalid and Esquinazi model[27] where there is inhomogeneous transport near the surface and in the Gd-implanted region. We find that the Hall resistance is nonlinear, and there is an apparent anomalous Hall resistance that does not saturate even at 7 T and is large at 100 K. This is likely to be a consequence of inhomogeneous transport near the surface of the crystal that leads to a nonlinear Hall resistance rather than being due to a real AHE.

We acknowledge funding from the Ministry of Science and Innovation (C05X0802, C08X1206, and VICX0808) and the MacDiarmid Institute. We thank Jibu Stephen, Simon Granville, Jerome Leveneur, and Shen Chong for their assistance with the MPMS and PPMS measurements.

---

*Corresponding author: J.Kennedy@gns.cri.nz

[1] T. Dietl, H. Ohno, F. Matsukura, J. Cibert, and D. Ferrand, Science **287**, 1019 (2000).

[2] J. M. D. Coey, M. Venkatesan, and C. B. Fitzgerald, Nat. Mater. **4**, 173 (2005).

[3] A. J. Behan, A. Mokhtari, H. J. Blythe, D. Score, X.-H. Xu, J. R. Neal, A. M. Fox, and G. A. Gehring, Phys. Rev. Lett. **100**, 047206 (2008).

[4] H. S. Hsu, C. P. Lin, H. Chou, and J. C. Huang, Appl. Phys. Lett. **93**, 142507 (2008).

[5] S. R. Shinde, S. B. Ogale, J. S. Higgins, H. Zheng, A. J. Millis, V. N. Kulkarni, R. Ramesh, R. L. Greene, and T. Venkatesan, Phys. Rev. Lett. **92**, 166601 (2004).

[6] Q. Xu, H. Schmidt, S. Zhou, K. Potzger, M. Helm, H. Hochmuth, M. Lorenz, A. Setzer, P. Esquinazi, C. Meinecke, and M. Grundmann, Appl. Phys. Lett. **92**, 082508 (2008).

[7] M. Khalid, M. Ziese, A. Setzer, P. Esquinazi, M. Lorenz, H. Hochmuth, M. Grundmann, D. Spemann, T. Butz, G. Brauer, W. Anwand, G. Fischer, W. A. Adeagbo, W. Hergert, and A. Ernst, Phys. Rev. B **80**, 035331 (2009).

[8] A. Sundaresan, R. Bhargavi, N. Rangarajan, U. Siddesh, and C. N. R. Rao, Phys. Rev. B **74**, 161306 (2006).

[9] G. Z. Xing, Y. H. Lu, Y. F. Tian, J. B. Yi, C. C. Lim, Y. F. Li, G. P. Li, D. D. Wang, B. Yao, J. Ding, Y. P. Feng, and T. Wu, AIP Adv. **1**, 022152 (2011).

[10] J. B. Yi, C. C. Lim, G. Z. Xing, H. M. Fan, L. H. Van, S. L. Huang, K. S. Yang, X. L. Huang, X. B. Qin, B. Y. Wang, T. Wu, L. Wang, H. T. Zhang, X. Y. Gao, T. Liu, A. T. S. Wee, Y. P. Feng, and J. Ding, Phys. Rev. Lett. **104**, 137201 (2010).

[11] P. Zhan, W. Wang, C. Liu, Y. Hu, Z. Li, Z. Zhang, P. Zhang, B. Wang, and X. Cao, J. Appl. Phys. **111**, 033501 (2012).

[12]T. P. Phan, Y. D. Zhang, D. S. Yang, N. X. Nghia, T. D. Thanh, and S. C. Yu, Appl. Phys. Lett. **102**, 072408 (2013).
[13]X. Xu, C. Xu, J. Dai, J. Hu, F. Li, and S. Zhang, J. Phys. Chem. C **116**, 8813 (2012).
[14]A. L. Schoenhalz, J. T. Arantes, A. Fazzio, and G. M. Dalpian, Appl. Phys. Lett. **94**, 162503 (2009).
[15]K. Sato, L. Bergqvist, J. Kudrnovsky, P. H. Dederichs, O. Eriksson, I. Turek, B. Sanyal, G. Bouzerar, H. Katayama-Yoshida, V. A. Dinh, T. Fukushima, H. Kizaki, and R. Zeller, Rev. Mod. Phys. **82**, 1633 (2010).
[16]M. Wei, N. Braddon, D. Zhi, P. A. Midgley, S. K. Chen, M. G. Blamire, and J. L. MacManus-Driscoll, Appl. Phys. Lett. **86**, 072514 (2005).
[17]M. Venkatesan, C. B. Fitzgerald, J. G. Lunney, and J. M. D. Coey, Phys. Rev. Lett. **93**, 177206 (2004).
[18]P. P. Murmu, J. Kennedy, G. V. M. Williams, B. J. Ruck, S. Granville, and S. V. Chong, Appl. Phys. Lett. **101**, 082408 (2012).
[19]X. Ma, Thin Solid Films **520**, 5752 (2012).
[20]A. A. Dakhel and M. El-Hilo, J. Appl. Phys. **107**, 123905 (2010).
[21]K. Potzger, S. Zhou, F. Eichhorn, M. Helm, W. Skorupa, J. Fassbender, T. Herrmannsdörfer, and A. Bianchi, J. Appl. Phys. **99**, 063906 (2006).
[22]M. Subramanian, P. Thakur, M. Tanemura, T. Hihara, V. Ganesan, T. Soga, K. H. Chae, R. Jayavel, and T. Jimbo, J. Appl. Phys. **108**, 053904 (2010).
[23]H. Shi, P. Zhang, S. S. Li, and J. B. Xia, J. Appl. Phys. **106**, 023910 (2009).
[24]V. Ney, S. Ye, T. Kammermeier, K. Ollefs, F. Wilhelm, A. Rogalev, S. Lebègue, A. L. da Rosa, and A. Ney, Phys. Rev. B **85**, 235203 (2012).
[25]I. Bantounas, S. Goumri-Said, M. B. Kanoun, A. Manchon, I. Roqan, and U. Schwingenschlögl, J. Appl. Phys. **109**, 083929 (2011).
[26]W. Dunhui, H. Songling, H. Zhida, S. Zhenghua, W. Yi, and D. Youwei, Solid State Commun. **131**, 97 (2004).
[27]M. Khalid and P. Esquinazi, Phys. Rev. B **85**, 134424 (2012).
[28]Ü. Özgür, Ya. I. Alivov, C. Liu, A. Teke, M. A. Reshchikov, S. Doğan, V. Avrutin, S.-J. Cho, and H. Morkoç, J. Appl. Phys. **98**, 041301 (2005).
[29]S. Lany and A. Zunger, Phys. Rev. Lett. **98**, 045501 (2007).
[30]M. Nistor, F. Gherendi, N. B. Mandache, C. Herbert, J. Perrière, and W. Selier, J. Appl. Phys. **106**, 103710 (2009).
[31]A. Singh, S. Chaudhary, and D. K. Pandya, Appl. Phys. Lett. **102**, 172106 (2013).
[32]M. Ungureanu, H. Schmidt, Q. Xu, H. von Wenckstern, D. Spemann, H. Hochmuth, M. Lorenz, and M. Grundmann, Superlattices Microstruct. **42**, 231 (2007).
[33]M. M. Parish and P. B. Littlewood, Phys. Rev. B **72**, 094417 (2005).
[34]S. Zhou, K. Potzger, Q. Xu, K. Kuepper, G. Talut, D. Markó, A. Mücklich, M. Helm, J. Fassbender, E. Arenholz, and H. Schmidt, Phys. Rev. B **80**, 094409 (2009).
[35]Q. Xu, H. Schmidt, H. Hochmuth, M. Lorenz, A. Setzer, P. Esquinazi, C. Meinecke, and M. Grundmann, J. Phys. D: Appl. Phys. **41**, 105012 (2008).